

Baltic Astronomy, vol. 18, 33–52, 2009

PHOTOMETRY AND CLASSIFICATION OF STARS AROUND THE REFLECTION NEBULA NGC 7023 IN CEPHEUS. II. INTERSTELLAR EXTINCTION AND CLOUD DISTANCES

K. Zdanavičius, J. Zdanavičius, V. Straizys and M. Maskoliunas
*Institute of Theoretical Physics and Astronomy, Vilnius University,
Goštauto 12, Vilnius, LT 01108, Lithuania*

Received 2009 May 20; accepted 2009 June 24

Abstract. Interstellar extinction is investigated in a 1.5 square degree area in the direction of the reflection nebula NGC 7023 at $\ell = 104.1^\circ$, $b = +14.2^\circ$. The study is based on photometric classification and the determination of interstellar extinctions and distances of 480 stars down to $V = 16.5$ mag from photometry in the *Vilnius* seven-color system published in Paper I (2008). The investigated area is divided into five smaller subareas with slightly different dependence of the extinction on distance. The distribution of reddened stars is in accordance with the presence of two dust clouds at 282 pc and 715 pc, however in some directions the dust distribution can be continuous or more clouds can be present.

Key words: stars: fundamental parameters, classification – Galaxy: Cepheus Flare, NGC 7023 – ISM: extinction, clouds: individual (TGU 629)

1. INTRODUCTION

The distances to star-forming regions in the Cepheus Flare, an out-of-plane concentration of interstellar dust and molecular clouds, are still unknown to sufficient accuracy, see the recent review by Kun et al. (2008). This our investigation is an attempt to determine more reliable distances and extinctions of dust clouds in the direction of the reflection nebula NGC 7023, illuminated by the young high-mass star HD 200775 and surrounded by the dust cloud TGU 629 (Dobashi et al. 2005).

In our earlier paper (Zdanavičius et al. 2008, hereafter Paper I) we determined in this area the magnitudes and color indices in the *Vilnius* seven-color photometric system for 1240 stars down to $V \approx 16.7$ mag. The published catalog for most of the stars also contains two-dimensional spectral types determined by interstellar reddening-free methods from the multicolor photometric data.

In the present paper we apply the classification results of Paper I for determining the distribution of the interstellar dust with distance in the 1.5 square degree area around the NGC 7023 nebula, using only the selected stars with the most reliable spectral types. In Section 2, we describe the classification methods based on the interstellar reddening-free parameters, used for determining the spectral types, and calculate interstellar reddenings and extinctions of the stars. The distribution

of interstellar dust in the area is investigated in Section 3 and the discussion and summary of the results are given in Section 4.

2. TWO-DIMENSIONAL PHOTOMETRIC CLASSIFICATION

For the classification of stars a few different codes using slightly different spectral standards were used.

1. COMPAR code is based on the σQ method described by Straizys et al. (1992, 2002). The method uses matching 14 different interstellar reddening-free Q -parameters of a program star to those of about 8400 standard stars of various spectral and luminosity classes, metallicities and peculiarity types. The results of the classification are spectral and luminosity classes and the indication of peculiarity. Several varieties of the code and sets of standards were used.

2. xqKLAS code uses the xq-method described by Zdanavičius (2005). The method is based on a new concept of reddening-free parameters (q) and a ‘virtual’ quantity of the interstellar dust (x). 1418 standards were formed by calculating the mean dereddened color indices for 89 spectral subclasses (in most cases, for each one subclass and for late-type stars for each 0.25 subclass) and the 17 values of the absolute magnitude, M_V . The results of the classification are spectral class and absolute magnitude.

3. TINKLAS code classifies stars using six Q, Q diagrams described in Straizys (1992) monograph. Each of them is formed from two reddening-free Q -parameters and calibrated in terms of spectral classes and absolute magnitudes. The results are spectral class and absolute magnitude.

Spectral classes and absolute magnitudes of stars determined by the methods (2) and (3) were used to estimate their luminosity classes taking the calibration of MK spectral types in absolute magnitudes from Straizys (1992). Then the spectral and luminosity classes determined by the three methods for each star were weighted and averaged. The intrinsic color indices used in determining the interstellar extinction and the distance are also taken from Straizys (1992).

As it was stated in Paper I, the $J-H$ and $H-K_s$ color indices from the 2MASS survey (Cutri et al. 2003; Skrutskie et al. 2006) in some cases were helpful for the identification of K and M dwarfs.

3. INTERSTELLAR EXTINCTIONS AND DISTANCES

The interstellar redshifts E_{Y-V} of 480 stars with the most reliable classification were determined as differences between the observed color indices $Y-V$ given in Table 2 of Paper I and the intrinsic color indices $(Y-V)_0$ for a given spectral type taken from Tables 67–69 of the Straizys (1992) monograph. Color excesses were transformed to extinctions by the equation $A_V = 4.16 E_{Y-V}$. Distances d to the stars in parsecs were calculated by the equation $5 \log d = V - M_V + 5 - A_V$. Here V are from Paper I and M_V are from the tabulation given in Straizys (1992, Appendix I), adjusted to a Hyades distance modulus of 3.3 mag. The results are given in Table 1 which gives the star number in the catalog of Paper I, V magnitude, spectral type and its quality, absolute magnitude M_V , interstellar extinction A_V , distance d and the name of the subarea to which the star is attributed. The subareas are described lower in this section and are shown in Figure 2.

Table 1. Stars in the investigated area with most reliable spectral types determined from *Vilnius* photometry. The column p gives the accuracy estimates of spectral types.

No.	V	Sp	p	M_V	A_V	d (pc)	Subarea
5	15.75	g2.5 V	1.0	4.59	1.36	910	I
6	12.91	g8 III	1.0	0.78	1.25	1500	I
11	15.77	f6 V	0.9	3.73	1.13	1520	I
12	15.39	f5 III	0.9	1.79	1.07	3200	I
14	15.70	k0.5 V	0.8	5.95	1.31	488	I
15	14.56	g0 IV	0.9	3.10	1.09	1190	I
16	15.29	g1 V	0.8	4.76	1.14	760	I
23	15.70	g7 V	1.0	5.40	1.00	720	I
33	13.70	f7 IV	0.9	2.10	1.11	1250	I
34	11.75	f8 V	0.9	3.84	0.24	342	I
40	15.62	g5.5 V	1.0	4.91	1.73	630	I
47	15.84	g2.5 V	0.8	4.85	1.18	920	I
50	12.56	g2 V	1.0	4.47	0.79	289	I
51	14.98	f8 IV	0.9	2.40	1.13	1950	I
53	13.65	f1 III	0.9	1.20	1.20	1780	I
54	15.41	g9 III	0.8	1.35	1.18	3760	I
56	15.68	g8 III	0.8	0.61	2.03	4060	
57	15.90	g7 V	1.0	5.24	1.12	810	I
63	14.33	k0 III	1.0	0.50	1.49	2950	IV
68	13.91	g8 V	1.0	5.35	0.84	350	I
71	15.26	f8 IV	0.9	2.22	1.14	2390	I
72	16.62	f7 V	0.7	4.07	1.16	1900	I
75	9.71	f5 IV	0.9	2.71	0.09	241	IV
76	12.40	f3 V	0.9	3.16	0.74	500	I
79	11.69	g1 V	0.8	4.59	0.00	263	I
82	15.19	g4 V	1.0	4.71	1.00	790	I
83	14.49	g1.5 V	1.0	4.48	0.41	830	I
84	13.90	f8 IV	0.9	1.96	1.51	1220	IV
86	15.59	f5 V	0.9	3.56	0.99	1610	I
87	13.38	g9.5 III	1.0	0.75	1.18	1950	I
88	14.39	f4 V	0.9	3.40	1.09	960	I
89	10.15	f3 V	0.9	3.24	0.01	240	I
101	13.82	g8 III	1.0	1.59	1.54	1370	IV
103	12.42	k2 III	1.0	0.70	1.05	1360	I
104	12.38	f4 III	0.9	1.96	1.31	660	IV
105	13.13	k1 IV	1.0	3.11	1.15	590	I
108	15.80	g3 V	0.8	4.87	1.06	940	I
110	15.71	g1.5 V	0.8	4.45	1.22	1020	I
117	15.19	g9.5 III	0.8	0.70	1.85	3380	IV
125	16.08	k1.5 V	0.7	6.37	0.86	590	I
126	14.99	f5 V	0.9	3.64	1.11	1120	I
134	14.69	f5 IV	0.9	2.23	1.66	1450	IV
135	14.59	g9 IV	1.0	2.64	1.48	1240	IV
136	14.63	k1.2 V	1.0	5.46	0.92	447	I
138	16.42	g3 IV	0.7	2.89	1.16	2980	I

Table 1. Continued

No.	V	Sp	p	M_V	A_V	d (pc)	Subarea
141	16.15	g1.5 IV	0.7	3.09	1.50	2040	I
143	15.41	k1 IV	0.8	3.64	1.38	1190	I
144	16.18	g3 IV	0.7	3.44	1.60	1690	IV
147	15.52	g8 V	1.0	5.01	1.19	730	IV
149	16.07	k0.5 IV	0.8	3.19	1.16	2210	I
150	14.98	k0.5 V	1.0	5.84	0.56	520	I
153	13.03	k3.5 III	1.0	0.48	1.07	1980	I
158	15.96	g9.5 IV	0.8	2.75	1.26	2450	I
160	14.45	a5 IV	0.9	1.24	1.78	1930	IV
161	11.60	g8 III	1.0	0.83	1.50	710	I
162	15.04	k0.5 V	1.0	5.63	0.79	530	I
168	13.30	g9.5 III	1.0	0.54	2.13	1340	IV
174	15.54	f6 IV	0.9	2.62	1.63	1820	I
176	16.14	g1 V	0.8	4.56	0.83	1410	I
177	15.61	g3 V	0.8	4.80	1.50	730	I
178	14.98	k0.5 IV	0.8	2.77	1.10	1660	I
179	13.79	f6 IV	0.9	2.85	1.27	860	IV
181	15.93	g2 V	0.8	4.70	1.29	970	I
182	13.11	g9 III	1.0	0.73	1.65	1400	IV
184	15.09	g1.5 IV	1.0	3.23	1.21	1340	I
185	15.32	k0 III	0.8	1.08	1.58	3400	IV
188	15.09	k3.2 III	0.8	0.73	1.25	4170	
190	9.80	k3 III	1.0	0.29	1.62	720	I
194	11.56	g3 V	1.0	4.82	0.15	209	IV
199	15.45	g1 IV	0.7	3.02	1.85	1310	IV
200	12.78	k0.7 III	1.0	0.79	1.67	1150	IV
202	15.58	g7 V	1.0	5.47	1.23	600	I
204	15.22	g0 V	1.0	4.00	1.45	900	IV
205	14.52	g3 V	1.0	4.87	1.08	520	I
207	13.08	g0 IV	0.9	2.54	0.97	820	IV
208	15.67	k1 IV	0.8	3.66	1.34	1370	IV
209	14.36	g3 V	1.0	4.86	0.86	530	I
215	12.61	f3 IV	0.9	2.54	0.83	710	I
216	15.68	g1.5 V	1.0	4.44	1.34	960	I
217	14.56	f8 IV	0.9	2.38	1.53	1350	IV
223	15.53	g5 IV	0.7	3.04	1.36	1680	I
225	14.50	g9 IV	1.0	3.48	1.15	940	I
226	16.47	f5 V	0.7	3.66	1.41	1900	IV
228	13.64	g8 IV	1.0	3.01	1.47	680	IV
231	15.02	g2 IV	1.0	3.02	1.63	1190	IV
233	15.41	k2.5 V	0.8	5.92	0.49	630	I
235	11.72	k0 III	1.0	0.72	1.16	930	IV
241	15.47	g6 III	0.7	1.01	2.15	2890	IV
242	13.66	g0 V	1.0	4.20	0.65	580	I
249	14.67	k0.5 III	0.8	0.59	1.93	2700	IV
250	14.49	k1.7 III	0.8	0.67	1.56	2820	IV
251	13.49	g2.5 V	1.0	4.40	1.09	400	I

Table 1. Continued

No.	<i>V</i>	Sp	<i>p</i>	<i>M_V</i>	<i>A_V</i>	<i>d</i> (pc)	Subarea
252	15.45	g9.5 V	1.0	5.36	1.20	600	IV
254	14.00	k3 V	0.8	6.63	0.71	214	IV
258	14.16	f7 IV	0.9	2.70	1.39	1030	IV
259	13.52	f7 V	0.8	3.71	0.67	670	I
266	7.70	k3 III	1.0	0.70	0.28	221	IV
267	14.98	g9 IV	1.0	3.51	1.43	1020	IV
274	15.78	g2 V	1.0	4.59	1.45	890	I
275	12.98	g5.5 III	1.0	0.71	1.54	1400	IV
277	15.06	g9.5 IV	0.8	2.90	1.70	1240	I
284	15.52	g8 V	1.0	5.20	1.36	620	I
285	12.51	g8 V	1.0	5.24	0.08	274	I
286	13.56	k3.5 III	0.8	0.45	1.75	1880	I
290	14.45	k0.7 IV	1.0	2.63	1.94	950	IV
292	15.35	g9 V	1.0	5.67	1.43	448	IV
293	14.97	f7 IV	0.9	2.37	1.21	1890	I
300	11.65	f6 III	0.9	2.00	0.76	600	I
301	14.19	g9.5 IV	1.0	2.48	1.32	1200	IV
302	12.51	f5 IV	0.9	1.77	1.19	820	IV
304	11.37	g6 V	1.0	5.14	0.13	165	IV
305	14.15	f6 IV	0.9	2.52	1.62	1010	IV
307	16.09	f8 V	0.8	4.15	1.11	1460	I
308	12.53	f7 IV	0.9	2.74	1.29	500	I
309	13.42	g5.5 V	1.0	4.83	0.74	371	I
310	15.51	k0.5 V	1.0	5.92	1.31	453	IV
312	14.74	k2 III	0.8	1.16	2.15	1930	IV
314	15.68	g3 V	0.8	4.71	1.46	800	IV
315	15.65	k0 V	0.8	5.77	1.32	520	IV
321	13.06	f0 IV	0.9	2.11	1.23	880	IV
323	14.12	f9.5 IV	0.9	2.94	1.36	920	IV
324	14.70	g1.5 IV	1.0	2.51	1.10	1660	IV
325	15.94	f7 V	0.7	3.94	2.09	960	IV
331	14.07	g9.5 IV	1.0	2.89	2.46	560	IV
333	15.26	f9 IV	0.9	2.36	1.44	1960	IV
335	15.81	f9.5 V	0.7	4.36	1.65	910	IV
337	15.35	f9.5 V	0.9	4.23	1.11	1000	I
339	13.78	k0 III	1.0	0.95	1.53	1820	IV
348	13.93	a8 III	0.9	1.02	1.29	2110	IV
349	14.48	g9.5 III	1.0	1.00	1.62	2350	I
350	15.55	f7 IV	0.9	2.68	2.02	1480	IV
351	11.44	g9 III	1.0	0.27	1.61	820	IV
352	15.35	f9 IV	0.9	2.71	1.92	1400	IV
353	15.25	g2.5 V	1.0	4.60	1.63	640	IV
356	12.41	k0.5 III	1.0	0.73	1.55	1060	IV
360	14.05	b7 V	1.0	-0.11	2.20	2460	IV
362	15.77	g0 V	0.8	4.45	1.57	890	IV
363	14.39	g9.5 IV	1.0	2.77	2.05	820	IV
369	12.68	f4 IV	0.9	2.38	0.97	740	IV

Table 1. Continued

No.	V	Sp	p	M_V	A_V	d (pc)	Subarea
373	14.02	g2.5 IV	1.0	3.01	1.68	740	IV
377	13.10	a7 IV	0.9	1.34	1.82	970	IV
378	15.20	k0.7 III	0.8	0.78	1.57	3710	IV
380	14.49	f7 V	0.9	3.95	0.85	870	I
383	14.87	k1.2 III	0.8	0.33	2.55	2500	IV
384	14.94	g1 V	0.9	4.25	1.23	780	IV
386	15.57	g4 V	1.0	4.77	1.24	820	
391	14.67	k7 V	0.8	8.15	0.00	201	I
394	15.21	g1 IV	1.0	2.81	1.51	1500	IV
395	12.55	g6 V	1.0	5.14	0.11	288	IV
398	15.45	f9 V	0.9	4.13	1.39	970	IV
400	13.51	f8 IV	0.9	2.68	1.01	920	IV
403	12.80	f3 III	0.8	1.60	1.46	890	IV
409	14.75	k5 V	1.0	7.16	0.45	268	IV
411	13.37	f8 IV	0.9	1.88	1.18	1150	IV
415	15.65	g1 IV	0.9	2.21	1.39	2560	IV
418	12.75	f1 IV	0.9	1.89	1.24	840	IV
422	15.23	g3 V	1.0	4.86	1.27	660	IV
423	15.65	g1 IV	0.5	3.04	1.76	1480	IV
424	14.68	f9 IV	0.9	1.49	1.51	2170	IV
426	11.18	f4 III	0.9	1.82	1.37	395	V
428	12.22	a5 IV	0.9	0.93	1.33	990	IV
431	13.33	k2.2 V	0.8	6.25	0.15	243	V
434	15.36	g2.5 IV	0.9	2.53	1.56	1800	IV
437	16.43	f7 V	0.7	3.91	1.60	1520	IV
439	10.70	f0 IV	0.9	1.84	1.04	366	IV
443	14.83	f7 IV	0.9	2.43	1.42	1570	IV
446	15.57	g6 IV	0.8	3.17	1.45	1550	IV
448	11.71	g9 III	1.0	0.73	1.56	770	IV
451	14.00	f7 IV	0.9	2.82	1.24	970	IV
456	15.60	k0 III	0.8	0.68	1.92	3990	IV
457	15.35	g0 IV	0.9	2.75	1.42	1720	IV
460	16.35	g2 V	0.7	4.44	1.50	1210	IV
464	14.96	m2.5 V	0.8	10.06	0.25	85	IV
466	16.55	g7 V	0.8	5.40	1.24	960	IV
469	14.49	k0 IV	1.0	3.56	1.27	860	IV
473	12.23	g0 V	0.9	4.33	0.18	349	V
476	13.74	g7 V	1.0	5.37	0.64	352	IV
477	12.57	f5 V	0.9	2.17	1.29	660	IV
480	13.74	k3.5 III	0.7	0.65	1.53	2060	
482	15.66	g6 III	0.8	0.85	2.10	3480	IV
485	13.09	k0.7 IV	1.0	3.12	0.94	640	I
494	16.24	g2.5 V	0.7	4.71	1.93	830	IV
495	15.22	g1 V	0.9	4.51	0.74	990	I
496	13.92	g1 IV	1.0	2.27	1.56	1040	IV
497	15.82	m2 V	0.8	7.37	1.83	211	IV
498	11.02	f4 V	0.9	3.45	0.14	307	V

Table 1. Continued

No.	<i>V</i>	Sp	<i>p</i>	<i>M_V</i>	<i>A_V</i>	<i>d</i> (pc)	Subarea
499	12.81	m0 III	1.0	-0.68	1.63	2360	IV
500	13.65	f9 IV	0.9	2.71	1.08	940	I
501	11.95	f3 IV	0.9	2.37	0.85	560	I
504	15.65	f8 IV	0.8	2.72	1.78	1700	V
506	15.15	k0.5 IV	0.8	3.26	1.39	1260	IV
511	16.31	f7 V	0.7	3.90	1.44	1560	I
513	16.00	f9.5 V	0.7	4.37	1.66	980	IV
514	15.98	g8 V	1.0	5.56	0.91	800	I
516	15.82	f6 V	0.7	3.94	1.98	960	IV
519	15.33	g5.5 V	1.0	3.05	1.42	670	IV
521	14.56	k2.5 V	0.8	6.45	0.67	309	I
523	12.54	k1.5 III	1.0	0.90	1.34	1150	IV
527	14.30	f6 V	0.9	3.26	1.14	950	I
531	15.71	f8 V	0.5	4.21	1.96	810	V
533	13.61	g0 IV	1.0	2.38	1.44	910	IV
537	16.18	k3 V	0.8	6.56	0.99	530	IV
538	15.91	g3 V	0.7	4.51	2.36	640	V
540	15.16	g9.5 V	1.0	5.55	0.86	560	I
541	13.20	k0.7 V	1.0	5.77	0.27	272	IV
544	12.27	g2 V	0.8	4.69	0.12	311	IV
545	15.50	f8 V	0.7	4.11	2.11	720	IV
554	12.86	k3 III	1.0	0.67	1.22	1560	I
560	14.89	f7 V	0.8	3.92	1.25	880	IV
562	14.30	g2.5 III	1.0	0.84	1.95	2000	V
563	14.04	k1 V	1.0	6.03	0.44	327	V
565	14.97	g5 V	1.0	4.81	1.25	610	IV
567	15.73	a9 IV	0.8	1.97	1.86	2400	V
569	13.99	k2.2 III	0.8	0.50	2.71	1430	V
570	14.10	k0 IV	1.0	2.82	1.13	1070	I
572	14.56	f6 V	0.7	3.79	1.00	900	I
574	12.44	k2.5 III	0.7	1.41	1.11	970	I
576	15.01	g8 III	0.8	0.89	3.07	1630	V
577	14.04	k0 V	0.8	6.02	0.50	320	V
578	16.23	g1.5 V	0.7	4.46	1.30	1240	I
581	15.48	f8 IV	0.9	2.37	1.49	2100	I
582	15.43	g7 III	0.8	0.71	1.57	4280	I
583	14.29	g1.5 V	0.8	4.64	0.80	590	I
595	13.18	k2 V	1.0	6.34	1.56	114	V
597	13.31	k0.5 IV	1.0	2.54	1.46	730	I
598	15.53	k2 V	0.8	6.26	0.85	483	I
602	16.56	f7 IV	0.7	2.21	1.86	3150	I
604	15.67	f9 IV	0.9	2.95	1.53	1730	IV
607	14.73	f7 IV	0.9	1.88	1.98	1490	IV
609	14.57	k1.2 V	1.0	5.47	1.63	314	V
611	9.11	m0 III	1.0	-0.66	1.10	540	I
615	14.96	a1 IV	1.0	0.47	1.51	3940	II
622	13.47	k0 III	0.7	0.38	2.57	1270	V

Table 1. Continued

No.	V	Sp	p	M_V	A_V	d (pc)	Subarea
623	14.17	k1 IV	0.8	2.54	1.75	950	II
626	12.83	f5 IV	0.9	2.36	1.73	560	V
632	11.82	k0.7 V	1.0	6.00	0.20	133	V
633	15.36	g8.5 V	1.0	5.66	1.50	437	V
634	13.95	g8.5 IV	1.0	3.16	1.44	740	II
636	14.57	k6 V	0.6	7.83	0.55	173	V
638	13.05	k1 V	1.0	6.12	0.18	224	II
640	9.76	k2.2 III	0.8	0.82	0.83	420	II
643	12.94	g4 V	1.0	4.94	0.30	346	II
644	16.15	g1 IV	0.7	3.76	1.68	1390	IV
649	12.10	k3.7 III	1.0	0.27	1.70	1070	II
652	13.82	k3.2 V	0.8	6.69	0.18	245	V
656	13.67	g4 V	1.0	4.55	0.70	485	II
657	12.95	k0 V	1.0	5.57	0.15	279	V
659	14.53	g9.5 III	0.8	1.23	1.98	1840	IV
660	11.67	g4 V	1.0	4.95	0.19	202	V
662	16.55	f8 V	0.7	3.84	1.78	1530	IV
669	14.23	f7 V	0.9	3.74	0.95	810	II
671	14.24	k1.2 III	0.8	1.07	2.20	1560	IV
674	15.54	g5 IV	1.0	3.48	1.22	1470	IV
676	16.05	g8 V	0.8	5.43	1.28	740	IV
682	14.06	g8 V	1.0	5.13	0.58	469	II
693	15.01	f3 V	0.6	3.14	2.53	740	V
694	14.28	f6 III	0.9	1.58	1.81	1510	IV
695	14.93	f6 IV	0.9	2.16	1.66	1660	IV
696	15.34	g8 V	1.0	5.06	0.84	770	IV
698	14.34	g9 III	1.0	0.71	1.89	2230	IV
700	12.58	f4 IV	0.9	2.56	0.73	720	II
703	13.86	f4 IV	0.9	2.43	1.09	1160	II
705	15.04	f7 IV	0.9	2.54	1.33	1710	II
706	15.75	f4 V	0.8	3.31	1.19	1780	II
708	11.81	f9 V	0.8	4.15	0.18	312	V
709	15.08	g6 V	1.0	4.92	0.82	740	II
710	15.85	f9.5 V	0.9	4.26	1.39	1100	IV
711	14.76	f8 IV	0.9	1.88	2.11	1420	IV
712	14.60	f8 IV	0.9	2.86	1.15	1310	IV
714	12.18	k2.7 V	1.0	6.47	0.29	121	V
719	15.21	f7 IV	0.9	2.00	1.29	2420	II
720	16.10	g1 V	0.7	4.45	1.76	950	IV
722	15.21	g2 V	1.0	4.67	0.44	1050	II
727	14.93	k0.5 V	1.0	5.89	0.73	460	II
731	12.66	k2 V	1.0	6.33	0.23	166	IV
738	15.76	g8 IV	0.8	2.65	1.90	1740	IV
739	16.01	k1.2 V	0.8	6.22	0.90	600	IV
742	15.61	g3 V	0.8	4.75	1.24	840	IV
750	14.49	f6 IV	0.9	2.69	1.54	1130	IV
754	11.69	k4.2 III	1.0	0.21	1.16	1160	II

Table 1. Continued

No.	<i>V</i>	Sp	<i>p</i>	<i>M_V</i>	<i>A_V</i>	<i>d</i> (pc)	Subarea
757	12.77	a5 IV	0.9	1.32	1.42	1010	IV
760	14.01	f6 IV	0.9	2.42	1.15	1220	IV
769	15.88	g4 V	1.0	5.02	1.34	800	IV
770	12.95	f8 IV	0.9	2.75	0.88	730	IV
775	16.36	g2 V	0.7	4.80	1.39	1080	IV
776	15.88	f6 III	0.7	1.54	2.13	2770	IV
778	13.81	f7 IV	0.9	2.73	0.95	1060	IV
780	14.27	k0 III	1.0	0.81	2.01	1940	IV
786	16.28	g0 IV	0.7	3.10	1.74	1940	IV
789	13.86	f7 IV	0.9	2.05	1.07	1400	IV
793	15.87	f9 V	0.8	4.04	1.39	1230	IV
797	14.05	f6 IV	0.9	2.60	1.39	1030	IV
798	14.35	k0.7 V	1.0	5.73	0.36	447	II
799	15.09	g5.5 III	1.0	0.80	1.58	3490	II
800	15.79	f4 III	0.7	1.92	2.02	2350	IV
803	14.71	f0 IV	0.9	2.02	1.51	1720	IV
804	14.04	g4 V	1.0	4.15	0.17	880	II
805	14.72	g9.5 V	1.0	5.63	0.84	447	IV
810	14.57	a8 IV	0.9	1.70	2.01	1490	IV
811	12.13	g2.5 IV	1.0	3.35	0.51	449	IV
812	15.53	g2.5 V	1.0	4.61	1.21	870	IV
814	15.96	f7 IV	0.7	2.48	1.93	2050	IV
815	16.01	g2 V	0.7	4.78	1.42	920	IV
820	14.63	g1 V	0.9	4.45	0.85	730	IV
821	8.99	f8 V	0.8	4.03	0.08	95	IV
823	15.93	k2.5 V	0.8	6.35	1.00	520	IV
825	13.74	g1.5 V	0.9	4.56	0.66	510	III
826	15.44	k1.2 V	1.0	5.72	1.00	560	IV
828	14.09	k0 IV	1.0	2.64	1.82	840	IV
831	11.42	f8 V	0.8	4.03	0.15	281	IV
835	14.94	f9 IV	0.9	2.10	1.42	1920	IV
839	14.33	f8 V	0.9	3.96	0.61	900	IV
844	13.03	g8 III	1.0	0.84	1.15	1610	II
846	14.70	f9 IV	0.9	2.10	1.54	1630	III
847	15.61	g1 V	1.0	4.41	0.94	1130	IV
855	15.71	g0 IV	0.9	2.57	1.51	2120	IV
857	13.53	f9 V	0.9	4.05	0.58	600	III
861	14.91	g0 IV	1.0	2.85	1.83	1110	II
868	12.05	g8.5 III	1.0	0.75	1.18	1060	IV
871	12.02	f7 IV	0.9	3.00	0.79	442	IV
876	15.34	f7 IV	0.8	2.27	1.73	1860	IV
881	14.76	f5 IV	0.9	2.63	1.37	1420	IV
887	11.51	g1 V	0.9	4.35	0.02	268	III
893	15.48	f8 V	0.8	3.91	1.09	1250	II
895	14.99	f4 V	0.9	3.49	0.96	1280	IV
896	14.10	k0.5 III	1.0	0.78	1.63	2190	IV
903	12.54	f8 IV	0.9	2.32	1.10	670	

Table 1. Continued

No.	V	Sp	p	M_V	A_V	d (pc)	Subarea
905	15.24	f9 V	0.9	4.08	0.67	1250	II
906	14.52	g4 V	1.0	5.07	0.79	540	II
910	13.79	f3 III	0.8	0.90	1.60	1810	III
911	13.69	f4 IV	0.9	2.44	1.12	1060	II
915	13.83	g1 IV	1.0	2.77	0.94	1060	II
917	15.52	g6 V	1.0	5.14	0.55	920	IV
923	14.53	g0 V	1.0	4.55	0.66	730	II
924	15.36	f7 IV	0.9	2.61	1.19	2050	II
925	14.64	a8 IV	1.0	1.66	1.76	1760	
926	15.93	f8 V	0.8	3.97	0.87	1660	II
928	13.04	k1.2 III	1.0	0.80	1.07	1710	II
932	14.03	g6 V	1.0	4.78	0.46	570	II
935	14.69	g4 V	1.0	4.74	0.57	750	III
936	14.21	g5.5 IV	1.0	2.41	1.38	1210	II
939	14.40	k0.5 V	1.0	5.84	0.59	392	II
943	13.06	g7 III	1.0	0.77	1.78	1260	III
946	13.48	g2 V	1.0	4.42	0.37	550	III
950	14.92	g3 V	1.0	4.86	0.57	790	II
952	11.49	f7 IV	0.9	2.52	0.37	530	III
953	11.40	f5 V	0.9	3.56	0.28	324	II
954	15.35	k2.7 V	1.0	6.58	0.77	398	III
956	10.90	g0 V	0.8	4.18	0.15	206	III
957	14.28	g0 V	0.8	4.35	0.68	710	II
958	15.95	g2.5 V	0.8	4.69	1.31	970	III
959	13.90	g3 IV	0.8	3.36	0.54	1000	II
962	16.10	f8 IV	0.7	1.85	2.11	2670	IV
963	13.38	k2.5 III	1.0	1.11	1.36	1520	IV
966	13.59	a8 IV	0.9	1.60	1.52	1240	
971	14.78	f5 IV	0.9	2.57	1.23	1570	II
972	12.51	g6 V	1.0	5.15	0.15	276	II
973	12.63	k0.5 III	1.0	0.10	1.85	1370	III
977	14.66	k1.7 V	0.8	6.09	0.35	440	II
978	15.32	f5 IV	0.9	2.68	1.38	1790	II
980	13.76	g1 V	0.9	4.41	0.54	580	III
983	14.85	k0.5 V	1.0	6.00	0.47	473	III
984	13.81	f8 IV	0.9	2.71	1.45	850	III
987	15.45	g9.5 V	1.0	5.54	0.89	640	III
988	14.11	f8 V	0.9	4.00	0.46	850	II
989	10.28	a7 V	0.9	2.29	0.60	300	II
991	15.13	g1.5 V	1.0	4.43	0.94	900	II
992	15.86	k2 V	0.7	6.40	0.78	550	IV
993	15.23	g8.5 IV	1.0	3.49	1.06	1370	II
995	14.48	g7 V	1.0	5.18	0.30	630	II
996	16.01	k1.2 V	0.8	5.51	0.35	1070	II
998	14.42	g8.5 V	1.0	5.56	0.53	463	II
1000	12.50	f5 V	0.9	3.50	0.52	495	III
1001	12.63	k0.5 V	1.0	5.74	0.09	229	II

Table 1. Continued

No.	<i>V</i>	Sp	<i>p</i>	<i>M_V</i>	<i>A_V</i>	<i>d</i> (pc)	Subarea
1007	15.04	g1 IV	0.9	3.12	0.77	1700	II
1010	14.74	k0 IV	1.0	2.73	1.30	1390	II
1012	11.77	g4 V	1.0	4.94	0.14	218	
1013	15.41	g9 III	0.8	1.22	1.81	2990	III
1017	14.86	f9 V	0.8	4.47	0.74	850	II
1018	11.54	f5 V	0.9	3.43	0.38	352	III
1020	16.67	f7 V	0.7	4.09	1.23	1860	II
1021	14.45	g8 III	1.0	0.88	2.06	2000	III
1023	14.21	g8.5 IV	1.0	3.17	1.16	950	II
1024	12.38	k5.5 V	0.8	7.37	0.22	91	III
1026	14.90	g8 IV	1.0	3.07	1.83	1000	III
1029	15.85	k2.7 V	0.8	6.52	0.59	560	II
1031	13.31	f8 IV	0.9	2.57	1.03	880	
1032	11.83	f8 IV	0.9	2.92	0.31	520	III
1033	13.68	k0.5 III	1.0	0.82	1.60	1780	III
1040	16.30	f9.5 V	0.8	4.40	0.98	1530	II
1041	15.39	g7 III	0.8	0.15	2.06	4320	III
1043	16.50	g4 V	0.7	5.20	1.14	1080	III
1044	15.28	k0.5 V	1.0	5.89	0.50	600	III
1047	14.74	f8 V	0.9	3.90	1.03	910	II
1054	14.68	f9 V	0.8	4.19	0.88	840	III
1055	13.96	g0 V	1.0	4.48	0.32	680	II
1056	14.68	k4.5 V	1.0	7.08	0.50	264	III
1059	16.12	g3 V	1.0	4.84	0.86	1210	II
1061	12.45	a8 V	0.9	2.45	0.74	710	III
1067	12.63	f0 III	0.9	1.37	1.06	1100	II
1070	13.93	g1.5 V	1.0	4.51	0.45	620	III
1071	11.32	k2.2 III	0.8	1.40	0.25	860	II
1074	14.29	k2.2 III	0.8	0.96	1.47	2360	II
1076	10.00	k0.5 III	1.0	0.52	0.42	650	II
1077	14.14	g8 III	1.0	1.10	1.44	2090	II
1078	15.90	k2 V	0.7	6.31	0.48	660	II
1081	13.57	g2 V	0.8	4.55	0.39	530	II
1087	15.58	k0 V	0.7	5.79	0.64	680	III
1089	15.04	f5 V	0.9	3.45	1.01	1310	II
1090	13.43	g5 V	1.0	5.03	0.43	393	II
1093	14.05	g5 V	1.0	4.95	0.51	520	III
1096	14.54	k1 III	0.8	1.02	1.72	2290	III
1101	15.68	k1.2 V	0.8	6.12	0.40	680	II
1102	11.35	g9.5 III	1.0	0.88	0.79	860	II
1105	15.83	g8 V	1.0	5.00	0.62	1100	II
1106	15.04	g5 IV	1.0	2.72	1.86	1240	III
1111	15.29	g9 V	1.0	5.79	0.44	650	III
1113	9.14	k0 IV	1.0	2.78	0.30	164	II
1114	13.87	f9 V	0.9	4.14	0.40	730	III
1116	14.54	g1 V	0.9	4.37	0.98	690	II
1117	14.68	k1.5 V	1.0	6.16	0.45	412	III

Table 1. Continued

No.	V	Sp	p	M_V	A_V	d (pc)	Subarea
1120	13.02	g1 IV	0.9	2.82	0.79	760	III
1122	15.74	g4 V	1.0	4.74	1.03	990	II
1123	15.39	g9.5 IV	0.8	3.47	1.60	1160	II
1125	14.29	f1 IV	0.9	2.09	1.34	1490	II
1130	12.20	a8 V	0.9	2.25	0.74	700	III
1131	14.56	k0.5 V	1.0	5.72	0.37	494	II
1134	13.54	f6 V	0.8	3.97	0.39	690	II
1135	13.40	k1 III	1.0	0.58	1.66	1700	II
1140	12.75	k3 III	1.0	0.27	1.91	1300	III
1141	12.86	g3 V	0.8	4.80	0.25	364	III
1144	14.69	k1 V	1.0	5.91	0.57	437	III
1145	15.67	g6 V	1.0	5.01	0.77	950	II
1148	16.01	k3 V	0.7	6.69	0.43	600	II
1149	11.90	g3 V	1.0	4.92	0.12	236	III
1152	15.14	k8 V	0.8	7.49	0.00	339	III
1153	8.09	f0 V	0.9	2.63	0.09	118	II
1155	14.88	k3.2 V	0.8	6.72	0.41	355	II
1157	11.76	a9 IV	0.9	2.00	0.63	670	II
1158	14.81	k0 IV	1.0	3.05	1.41	1170	II
1161	13.76	f9 V	0.8	4.26	0.30	690	II
1162	12.28	g0 V	0.8	4.20	0.31	359	II
1163	14.44	k0 V	1.0	5.91	0.25	453	III
1164	14.99	k0.7 V	1.0	5.66	0.37	620	II
1166	15.76	f3 V	0.8	3.16	1.54	1630	II
1168	16.20	f1 V	0.8	2.95	1.65	2090	II
1170	15.39	k3 V	0.8	6.64	0.27	497	II
1173	12.62	f3 V	0.9	3.16	0.44	640	II
1175	13.24	g8.5 IV	1.0	3.66	0.43	670	II
1177	15.09	g2 V	0.8	4.67	1.15	710	III
1178	14.79	f6 V	0.8	3.92	0.86	1000	II
1180	14.45	f9.5 IV	0.9	2.18	1.08	1730	II
1183	15.91	g1 V	0.8	4.58	0.84	1250	II
1186	14.58	g5 V	1.0	4.84	0.60	670	II
1187	14.55	g2 V	0.9	4.71	0.41	770	III
1188	14.58	g1.5 V	1.0	4.51	0.31	900	II
1190	14.93	f6 IV	0.9	2.43	1.56	1540	III
1194	15.76	k2.5 V	0.8	6.49	0.32	610	II
1202	13.91	g0 V	1.0	4.30	0.79	580	II
1203	13.74	g0 V	0.9	4.28	0.38	650	II
1205	15.02	f8 V	0.8	4.15	1.38	790	II
1209	15.43	k0 V	1.0	5.90	0.68	590	III
1214	12.51	k0.5 III	1.0	1.06	1.34	1050	II
1215	13.29	g9.5 III	1.0	0.75	1.46	1650	II
1217	14.63	g9.5 V	1.0	5.49	0.29	590	II
1218	15.95	f9 V	0.9	4.07	1.28	1320	II
1219	16.01	k3 V	0.8	6.53	0.40	660	II
1221	10.54	f0 IV	0.9	2.14	0.28	421	II

Table 1. Continued

No.	<i>V</i>	Sp	<i>p</i>	<i>M_V</i>	<i>A_V</i>	<i>d</i> (pc)	Subarea
1222	14.49	g0 V	0.9	4.21	0.39	950	II
1224	15.94	k3 V	0.8	6.50	0.47	620	II
1225	15.32	g2 V	0.8	4.67	0.62	1010	II
1226	12.63	g1 V	0.9	4.31	0.23	414	II
1227	13.32	g5.5 V	1.0	5.10	0.37	372	II
1228	14.31	g7 V	1.0	5.23	0.65	486	II
1233	14.78	f9.5 V	0.8	4.39	0.29	1050	II
1236	12.95	g1.5 V	1.0	4.42	0.37	427	II
1238	15.84	k3.5 V	0.7	6.89	0.51	488	II
1239	12.99	f8 V	0.9	3.95	0.29	560	II
1240	13.63	g1 V	0.8	4.56	0.22	590	II
1243	13.67	g3 V	1.0	4.70	0.31	540	II

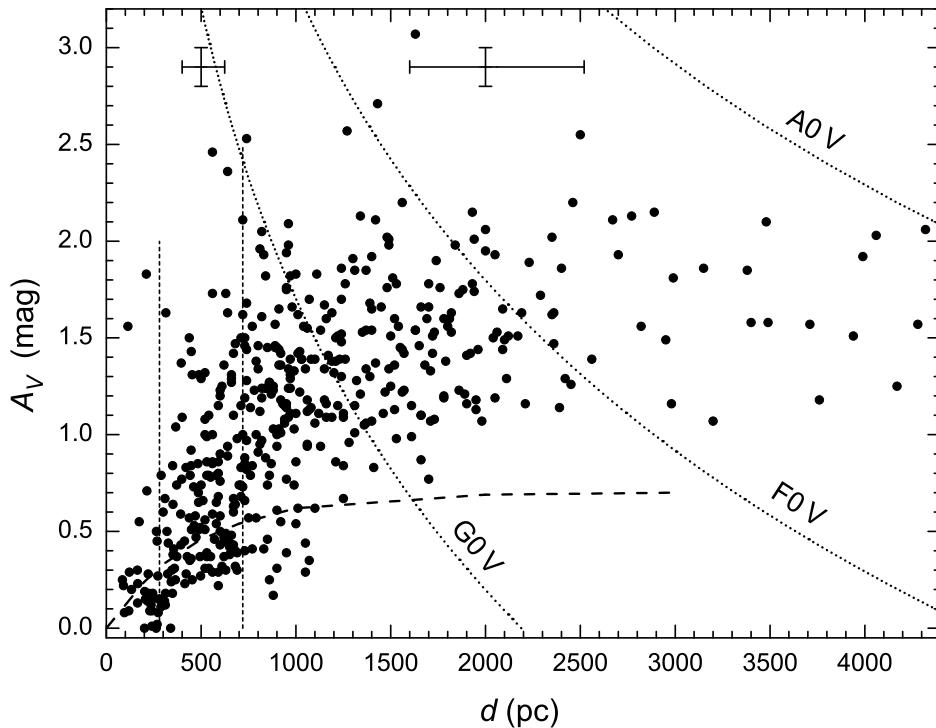


Fig. 1. Dependence of the A_V extinction on distance in the whole area. The three dotted curves show the limiting magnitude effect for A0 V, F0 V and G0 V stars. The curve at the right-hand upper corner is also valid for K0 III stars since their absolute magnitudes are close to those of A0 V stars. The lower segmented curve is the dependence of the extinction on distance for the Galactic latitude $+14.2^\circ$ calculated by the Parenago formula (see the text). The error bars correspond to standard deviations of the distance and the extinction at 0.5 kpc and 2 kpc distances. The two vertical lines mark the mean distances of the clouds.

Figure 1 shows the plot A_V vs. d for stars in the whole area. The three dotted curves correspond to A0 V (or K0 III), F0 V and G0 V stars at the limiting magnitude $V_{\text{lim}} = 16.0$. The stars of these spectral types (and absolutely fainter) above the corresponding curves are affected by the limiting magnitude, i.e., stars with high extinctions are missing at these distances. Consequently, the plot cannot be used for estimating both the mean and the maximum extinctions. However, up to a distance of 1 kpc all the stars absolutely brighter than G0 V are well represented in the areas where A_V is smaller than ~ 2 mag. At $d = 1$ kpc and $A_V = 2$ mag, only G, K and M dwarfs near the limiting magnitude are missing. In the upper part of Figure 1 the error bars of the distance and A_V are shown for the two distance values. They correspond to an error of ± 0.1 mag in A_V , ± 0.5 mag in M_V and $(-20, +26)\%$ in the distance.

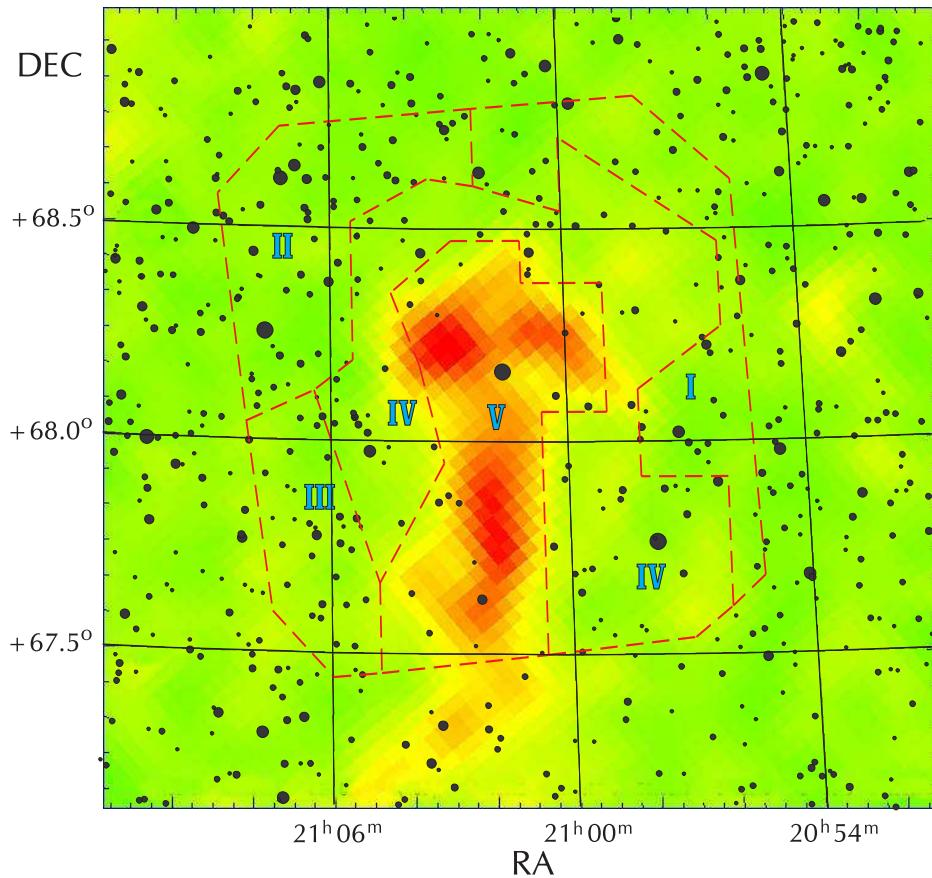


Fig. 2. The division of the investigated area into five subareas exhibiting slightly different dependencies of A_V on distance. The extinction map from Dobashi et al. (2005) atlas and the stars down to $V = 14$ from GSC are shown in the background.

The segmented curve in Figure 1, which starts from the origin of the coordinates, corresponds to the exponential extinction law for the Galactic latitude $b = +14.2^\circ$, calculated by the Parenago formula with the extinction coefficient $A_V = 1.5$ mag/kpc and the half-thickness of the dust layer $\beta = 0.11$ kpc (Parenago 1945; Sharov 1963; Straižys 1992, p. 146). It is evident that the Parenago curve is in agreement with the positions of low-extinction stars located closer to us than 500–700 pc.

For determining the distance to a dark cloud we usually use stars situated at a steep rise (or jump) of the extinction at the front edge of the cloud. However, some of these stars can have negative distance errors which originate mainly from the errors in their absolute magnitudes. Consequently, the true distance to the cloud can be larger than the distance corresponding to the jump defined by the stars apparently closest to the Sun. The true distance can be found as $d = d(\text{front}) + 0.2d$, or $d = d(\text{front}) / 0.8$, where $0.2d$ is the negative distance error when the error of the absolute magnitude $\Delta M_V = +0.5$.

However, the described situation takes place only in the case when a statistically significant number of stars at the extinction jump is available. In our case, at the expected cloud distance we have only a few stars with large extinctions. It is quite possible that some of them really have a negative error of the distance but it is also possible that their distance error happens to be zero or even positive, and we have no reason to apply the above described correction to their apparent distances. A more realistic value of the cloud distance can be obtained by averaging distances of the reddened stars in the interval between $d - 0.20d$ and $d + 0.26d$ where d is the true cloud distance.

In Figure 1 we can see that at ~ 250 pc a steep rise in the extinction takes place. However, two of the stars, Nos. 595 and 636 in the catalog of Paper I, exhibit too large extinction values, $A_V = 1.56$ and 0.55 mag, at small distances, 114 pc and 173 pc, respectively. The first of these two stars will be discussed below in this section. Both stars are excluded from determining the cloud distance. The remaining 10 stars with distances between 210 and 330 pc and $A_V \geq 0.5$ mag have the mean distance 282 ± 42 pc (standard deviation) which may be considered as the distance of the nearest cloud. This result should be considered as more accurate than the value of distance found by Straižys et al. (1992) applying a similar method for only four stars of magnitudes 11–12. Two of them in our Paper I were suspected as binaries.

At distances larger than 250 pc the extinction continues to rise almost up to 1 kpc. However, the presence of another jump (or jumps) of the extinction can be suspected. The most probable jump is observed between 560 and 875 pc, where 560 pc is the distance to the front edge, and the distance range is defined by $d - 0.20d$ and $d + 0.26d$. Within this distance range we have 10 stars with $A_V \geq 1.8$ mag. Their mean distance is 715 ± 110 pc (standard deviation).

Trying to better understand the extinction vs. distance relation, we have split the investigated field into five subareas with the boundaries shown in Figure 2 and with the extinction map from the Dobashi et al. (2005) atlas and the stars down $V = 14$ mag from the GSC catalog plotted in the background. Each of these subareas exhibits a somewhat different form of the A_V vs. distance dependence. In the following, the results of the extinction dependence on distance in these subareas will be described.

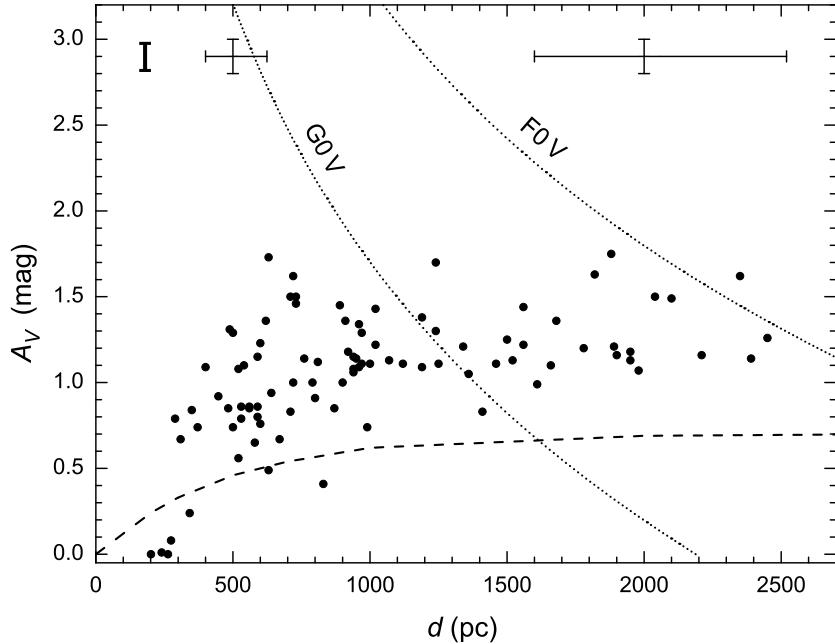


Fig. 3. The same as in Figure 1 but for Subarea I.

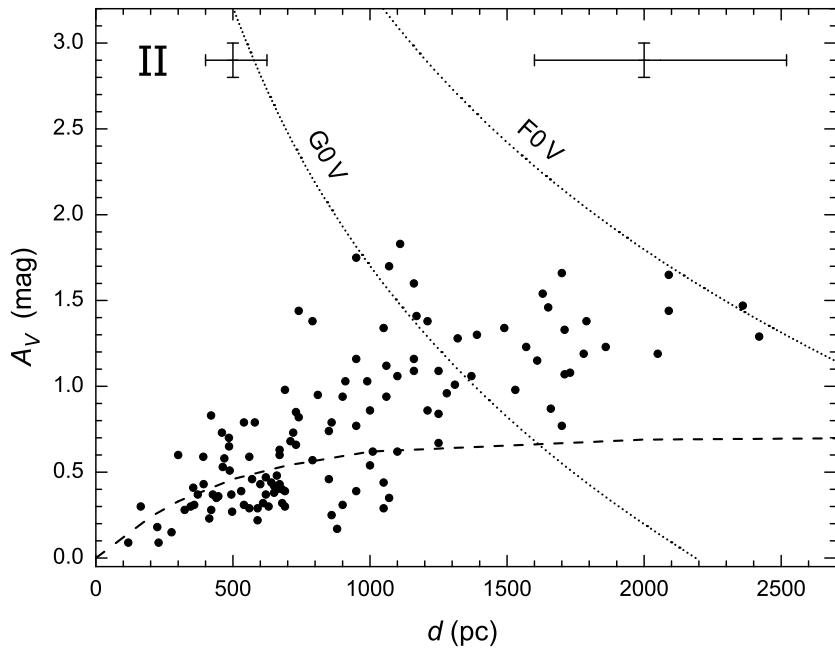


Fig. 4. The same as in Figure 1 but for Subarea II.

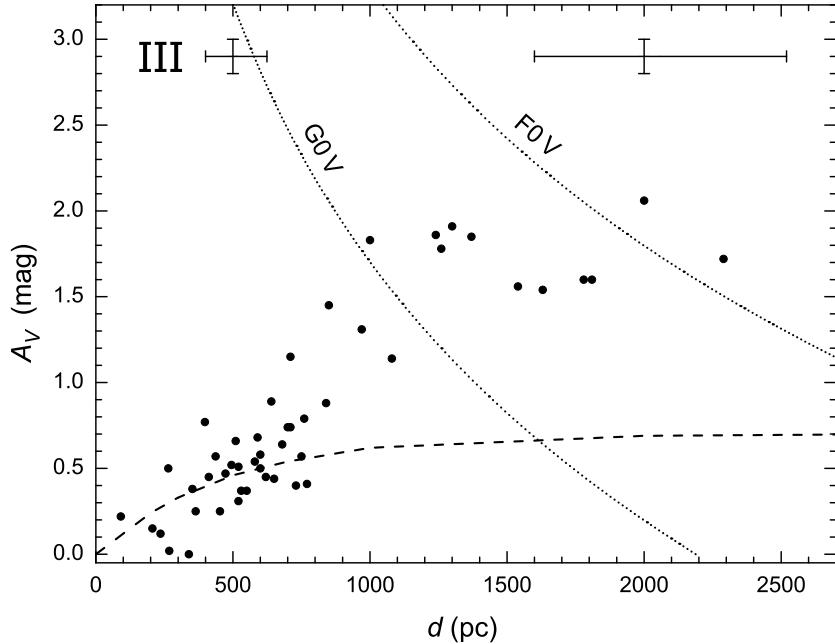


Fig. 5. The same as in Figure 1 but for Subarea III.

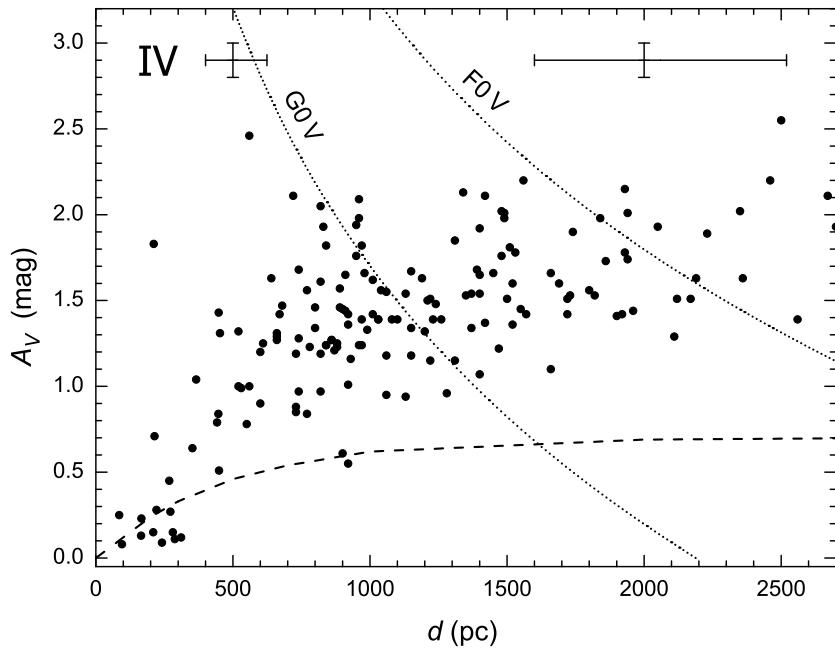


Fig. 6. The same as in Figure 1 but for Subarea IV.

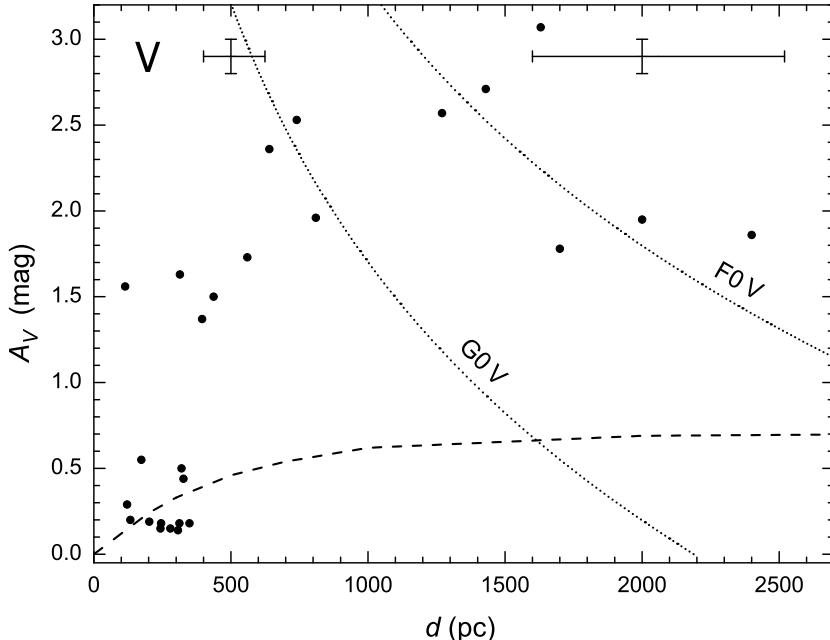


Fig. 7. The same as in Figure 1 but for Subarea V.

Figure 3 shows the A_V vs. d plot for Subarea I located along the right edge of the field. The first two reddened stars with A_V between 0.6–0.8 mag are seen at an apparent distance of ~ 290 pc, i.e., quite close to the mean distance of the first cloud estimated from Figure 1. A few more jumps between 500 pc and 750 pc are also possible. The mean extinction value at distances > 1.0 kpc is about 1.3 mag, and the maximum value is close to 1.75 mag.

Figure 4 shows the A_V vs. d plot for Subarea II located at the left upper corner of the area. Here, the nearest considerably reddened star is found at the apparent distance 300 pc, and the second jump is seen at ~ 700 pc. At $d > 1$ kpc the extinction remains more or less constant with a mean value of 1.3 mag. In this subarea a group of about 12 stars at a distance of 800–1100 pc exhibits quite low extinction, with the values between 0.2 and 0.6 mag. Probably, these stars are seen in the directions of relatively transparent windows. They are scattered over the whole subarea.

Figure 5 shows the A_V vs. d plot for Subarea III located at the lower left corner of the field. The positions of the two extinction jumps here cannot be estimated reliably but the height of the second jump is almost 1 mag, giving a mean extinction of 1.8 mag at $d > 1$ kpc.

Figure 6 shows the A_V vs. d plot for Subarea IV which surrounds the central dark cloud on three sides. The extinction jumps are close to the distances observed in other subareas. The extinction values show a considerable scatter (between 1.0 and 2.2 mag), with the mean value being about 1.6 mag. Two stars in the subarea exhibit the extinction values around 2.5 mag.

In Figure 7 we show the A_V vs. d plot for Subarea V which includes the darkest segment of the dust cloud with the reflection nebula NGC 7023. Only 14 classified stars with $A_V > 1.0$ have been found in this direction. Among these the most interesting is the above-mentioned star No. 595. Its photometric spectral type is K2 V, $V = 13.18$, $A_V = 1.56$ and $d = 114$ pc. It is strange to find this large extinction at such a small distance. The classification of the star by all of the methods applied is of good accuracy and coinciding. The small apparent distance of the star can be explained by its possible duplicity. If it is a binary with two identical components, the combined absolute magnitude should be more negative by 0.75 mag and the distance larger by a factor of 1.41, i.e., $114 \times 1.41 = 161$ pc, which is more realistic than the value for a single star, but still too small compared to the cloud distances in other subareas.

Other stars in Subarea V classified in Paper I are too scanty to estimate cloud distances. However, their distribution in the plot (Figure 7) is not in contradiction to the apparent distances of the two clouds at 282 pc and 715 pc. The largest extinction found in Subarea V is close to 3 mag, but this is not the real maximum value since the stars with larger extinctions are absent in our sample due to the limiting magnitude effect. With the help of 2MASS photometry we have found in this area a few red giants having $A_V \approx 15$ mag.

4. DISCUSSION AND CONCLUSIONS

The dust cloud TGU 629, surrounding the reflection nebula NGC 7023, belongs to a giant dust and molecular cloud system known as the Cepheus Flare. In the summaries of distance determinations of different objects in this system, Kun (1998) and Kun et al. (2008) came to the conclusion that the system either has a considerable depth or consists of several layers with distances ranging from 200 to 500 pc. Two layers of interstellar gas were found by radio observations by Heiles (1967) in the neutral hydrogen 21 cm line and by Grenier et al. (1989) in the CO molecular lines. Applying the kinematical method to velocity profiles of the lines, Grenier et al. find the approximate distances to the layers: 300 and 800–900 pc.

Our results described in Section 3 also give evidence that dust clouds in the vicinity of NGC 7023 concentrate at least in two layers at 282 pc and 715 pc. There is a possibility that the true distances of these cloud layers are not the same throughout the area. However, the number of stars at the extinction jumps in different subareas is too small to be sure that these distance differences are real. The extinction vs. distance plots also allow to suspect that more clouds are present along the line of sight. This is in agreement with the map of the CO intensity distribution (Dame et al. 2001) which evidences that the molecular cloud structure in the Cepheus Flare is quite clumpy and fragmented.

Our estimates of cloud distances are in satisfactory agreement with those found by Grenier et al. (1989) from kinematics of the CO clouds. The CO radial velocities show that at the Galactic longitude $\ell = 104^\circ$ both clouds are connected by a bridge. The distant CO layer should be more prominent at larger Galactic longitudes, i.e., on the left side of our area (Subareas II, III and, partly, IV). This is in agreement with our results.

If we accept that dust clouds in this direction reach a distance of 700 pc, the depth of the cloud layer should be about 400 pc. The length of the whole Cepheus Flare cloud system ($\sim 18^\circ$) corresponds to ~ 95 pc at a distance of 300 pc and to ~ 220 pc at a distance of 700 pc. It seems possible that the Cepheus Flare has its

extension known as the Polaris Flare (Heithausen et al. 1993; Dame et al. 2001). In this case the whole complex of molecular clouds from $\ell, b = (100^\circ, +14^\circ)$ to $(126^\circ, +30^\circ)$ has a length of $\sim 30^\circ$ and the projected complex length is from ~ 160 pc at a distance of 300 pc to ~ 375 pc at a distance of 700 pc. The apparent width of the Cepheus and Polaris Flares is only $\sim 8^\circ$, which corresponds to 42 pc at a distance of 300 pc and 100 pc at 700 pc.

The projected length of the cloud system at 700 pc (375 pc) is comparable to the observed depth of the complex (400 pc), i.e., the complex looks like a pancake, and our line of sight runs along its plane. The heights of the two cloud layers above the Galactic plane in the direction of NGC 7023 are 75 pc and 170 pc.

To have the estimates of cloud distances more accurate, one must minimize the errors of absolute magnitudes of the stars which define the jumps in the extinction vs. distance dependence. This can be done either by spectral observations of these stars to verify their spectral and luminosity classes or by determining trigonometric parallaxes. Within a few years, in the case of the success of the *Gaia* mission, the distance problem of these reddened stars will be solved.

ACKNOWLEDGMENTS. We are thankful to Edmundas Meištas and Stanislava Bartasiute for their help in preparing the paper. The use of the SkyView, Simbad, Gator and 2MASS databases is acknowledged.

REFERENCES

- Cutri R. M., Skrutskie M. F., Van Dyk S., Beichman C. A. et al. 2003, *2MASS All Sky Catalog of Point Sources*, NASA/IPAC Infrared Science Archive,
<http://irsa.ipac.caltech.edu/applications/Gator/>
- Dame T. M., Hartmann D., Thaddeus P. 2001, ApJ, 547, 792
- Dobashi K., Uehara H., Kandori R., Sakurai T., Kaiden M., Umemoto T.,
 Sato F. 2005, PASJ, 57, S1
- Grenier I. A., Lebrun F., Arnaud M., Dame T. M., Thaddeus P. 1989, ApJ, 347, 231
- Heiles C. 1967, ApJS, 15, 97
- Heithausen A., Stacy J. G., de Vries H. W., Mebold U., Thaddeus P. 1993, A&A, 268, 265
- Kun M. 1998, ApJS, 115, 59
- Kun M., Kiss Z. T., Balog Z. 2008, in *Handbook of Star Forming Regions*,
 ed. B. Reipurth, ASP, vol. 1, p. 136
- Parenago P. P. 1945, AZh, 22, 129
- Sharov A. S. 1963, AZh, 40, 900 = Soviet Astron., 7, 689
- Skrutskie M. F., Cutri R. M., Stiening R., Weinberg M. D. et al. 2006, AJ, 131, 1163
- Straižys V. 1992, *Multicolor Stellar Photometry*, Pachart Publishing House,
 Tucson, Arizona
- Straižys V., Černis K., Kazlauskas A., Laugalys V. 2002, Baltic Astronomy, 11, 219
- Straižys V., Černis K., Kazlauskas A., Meištas E. 1992, Baltic Astronomy, 1, 149
- Zdanavičius K. 2005, Baltic Astronomy, 14, 104
- Zdanavičius K., Zdanavičius J., Straižys V., Kotovas A. 2008, Baltic Astronomy, 17, 161 (Paper I)